provide critical information and a feedback mechanism for growth studies designed to establish rational pathways for controllably producing IMJs in the future.

References and Notes

1. S. Saito, *Science* **278**, 77 (1997).
2. P. L. McEuen, *Nature* **393**, 15 (1998).
3. C. Dekker, *Phys. Today* **52**, 22 (May 1999).
4. B. I. Dunlap, *Phys. Rev. B* **49**, 5643 (1994).
5. Ph. Lambin, A. Fonseca, J. P. Vigneron, J. B. Nagy, A. A. Lucas, *Chem. Phys. Lett.* **245**, 85 (1995).
6. L. Chico, V. H. Crespi, L. X. Benedict, S. G. Louie, M. L. Cohen, *Phys. Rev. Lett.* **76**, 971 (1996).
7. J.-C. Charlier, T. W. Ebbesen, Ph. Lambin, *Phys. Rev. B* **53**, 11108 (1996).
8. L. Chico, L. X. Benedict, S. G. Louie, M. L. Cohen, *Phys. Rev. B* **54**, 2600 (1996).
9. R. Saito, G. Dresselhaus, M. S. Dresselhaus, *Phys. Rev. B* **53**, 2044 (1996).
10. J. Han, M. P. Anantram, R. L. Jaffe, J. Kong, H. Dai, *Phys. Rev. B* **57**, 14983 (1998).
11. Z. Yao, H. W. Ch. Postma, L. Balents, C. Dekker, *Nature* **402**, 273 (1999).
12. P. G. Collins, A. Zettl, H. Bando, A. Thess, R. E. Smalley, *Science* **278**, 100 (1997).
13. J. W. G. Wildoer, L. C. Venema, A. G. Rinzler, R. E. Smalley, C. Dekker, *Nature* **391**, 59 (1998).
14. T. W. Odom, J.-L. Huang, P. Kim, C. M. Lieber, *Nature* **391**, 62 (1998).
15. ———, *J. Phys. Chem. B* **104**, 2794 (2000).
16. For example, a recent STM study suggests that the bend in a SWNT tube is an IMJ [L. C. Venema *et al.*, *Phys. Rev. B* **62**, 5238 (2000)]. However, the absence of atomic resolution makes it impossible to distinguish whether the observed "kink" connects two different tubes rather than corresponding to a simple bend. In addition, the VHS peaks above and below the bend are not consistent with the SWNT diameters. Hence, it is possible that the observed spectroscopic features are due to effects of bending (*15*).
17. T. W. Odom, J.-L. Huang, P. Kim, M. Ouyang, C. M. Lieber, *J. Mater. Res.* **13**, 2380 (1998).
18. M. Ouyang, J.-L. Huang, C. M. Lieber, unpublished data.
19. V. Meunier, P. Senet, Ph. Lambin, *Phys. Rev. B* **60**, 7792 (1999).
20. V. Meunier, Ph. Lambin, *Phys. Rev. Lett.* **81**, 5588 (1998).
21. D. Orlikowski, M. B. Nardelli, J. Bernholc, C. Ronald, *Phys. Rev. Lett.* **83**, 4132 (1999).
22. A. Rubio, *Appl. Phys. A* **68**, 275 (1999).
23. D. Orlikowski, M. B. Nardelli, J. Bernholc, C. Roland, *Phys. Rev. B* **61**, 14194 (2000).
24. M. S. Dresselhaus, G. Dresselhaus, P. C. Eklund, *Science of Fullerenes and Carbon Nanotubes* (Academic Press, San Diego, 1996).
25. P. Kim, T. W. Odom, J.-L. Huang, C. M. Lieber, *Phys. Rev. Lett.* **82**, 1225 (1999).
26. Preliminary tight-binding calculations for these two models do not exhibit good agreement with experiment (*18*).

27. We thank M. S. Gudiksen, T. W. Odom, H. Park, and P. Kim for helpful discussion. Supported by the NSF.

11 September 2000; accepted 21 November 2000

Evidence for Coherent Proton Tunneling in a Hydrogen Bond Network

Anthony J. Horsewill,[1]* Nicholas H. Jones,[1] Roberto Caciuffo[2]

We observed coherent proton tunneling in the cyclic network of four hydrogen bonds in calix[4]arene. The tunneling frequency of 35 megahertz was revealed by a peak in the magnetic field dependence of the proton spin-lattice relaxation rate measured with field-cycling nuclear magnetic resonance in the solid state at temperatures below 80 kelvin. The amplitude of the coherent tunneling peak grows with temperature according to a Boltzmann law with energy $D/k_B = (125 \pm 10)$ kelvin (where k_B is Boltzmann's constant). The tunneling peak can be interpreted in the context of level crossings in the region where the tunneling frequency matches the proton Larmor frequency. The tunneling spectrum reveals fine structure that we attribute to coupling between the hydrogen bonds in the network. The characteristics of the tunneling peak are interpreted in the context of the potential energy surface experienced by the hydrogen atoms in the network.

Quantum tunneling can occur when a particle with energy E encounters a potential barrier of magnitude V_0 greater than E. The tunneling probability that defines the tunneling frequency is an exponential function of the barrier properties and the particle mass, and so observations of tunneling are usually confined to particles of low mass that move over short distances.

The explicit observation of molecular tunneling has been confined to relatively few systems. For example, the rotation of symmetrical groups at low temperature and, in the life sciences, evidence for the role of hydrogen tunneling in enzyme catalysis have recently been revealed through the effects of the atomic mass on the rates of reaction by isotopic substitution (*1*, *2*).

Here we report the direct observation of coherent tunneling associated with proton transfer among a network of four coupled hydrogen (H) bonds in which the proton motion exhibits an oscillatory motion with a well-defined frequency. The coupling between H bonds also manifests itself in fine structure. These observations not only provide an example of coherent translational tunneling but also promise to reveal insight into the fundamental mechanisms of chemical reactions.

In selecting molecules with structural properties that are liable to reveal coherent tunneling, it is important to identify structures that, in the isolated molecule at least, have degenerate tautomers that can interconvert by proton motion. To minimize coupling to the environment that would otherwise quench the oscillatory modes, the energy asymmetry of the tautomers, which can then only arise from the interactions between molecules in the solid state, must be small. Calix[n]arenes can meet this requirement; they are bowl-shaped macromolecules with ordered arrays of phenol-methylene oligomers (*3*). We studied one of the simplest members of this family, calix[4]arene (Fig. 1). The molecule has fourfold symmetry, and its shape is maintained by a cyclic network of four intramolecular H bonds at its base. There are no intermolecular H bonds. We can identify two degenerate tautomers of the isolated molecule that are related by proton transfer among the four H bonds.

Nuclear magnetic resonance (NMR) relaxometry is well established for studying molecular dynamics. Atomic motion modulates the dipole-dipole interaction between nuclei and, indirectly, drives the population changes in the nuclear spin levels that give rise to spin-lattice relaxation. As the dipolar interaction has nuclear spin operators that involve one-spin ($m = 1$) and two-spin flips ($m = 2$), the spin-lattice relaxation rate, T_1^{-1}, simultaneously samples the spectral density at the Larmor frequency, ω_L, and twice the Larmor frequency. For a nucleus with spin I and magnetogyric ratio γ (*4*, *5*),

$$T_1^{-1}(\omega_L) = \frac{3}{2}\gamma^4\hbar^2 I(I+1) \times [J^{(1)}(\omega_L) + J^{(2)}(2\omega_L)] \qquad (1)$$

where $\hbar$ is Planck's constant divided by π. The spectral density, $J^{(m)}(\omega)$, is the Fourier transform of the dipolar correlation function:

$$J^{(m)}(\omega) = \int_{-\infty}^{\infty} \langle F^{(m)*}(t+\tau)F^{(m)}(t)\rangle \exp(i\omega\tau)d\tau \qquad (2)$$

where $i = \sqrt{-1}$ and $F^{(m)}$ is the spatial part of the proton dipolar interaction, which depends

---

[1] School of Physics and Astronomy, University of Nottingham, Nottingham, NG7 2RD, UK. [2] Istituto Nazionale per la Fisica della Materia, Università di Ancona, Dipartimento di Scienze dei Materiali e della Terra, Via Brecce Bianche, I-60131 Ancona, Italy.

*To whom correspondence should be addressed. E-mail: A.Horsewill@nottingham.ac.uk

on the relative positions of the nuclei at times t and $t + \tau$. $F^{(m)}$ is therefore modulated in time. When the dynamical process giving rise to the fluctuations is stochastic, the correlation function is an exponential decay and the spectral density function is a Lorentzian centered at zero frequency. When the dynamics are oscillatory, as would be the case for coherent tunneling, then the spectral density is a peak centered at the oscillation frequency. If the spin-lattice relaxation is measured as a function of magnetic field, B, the resulting plot of T_1^{-1} versus Larmor frequency, $\omega_L = \gamma B$, maps out the spectral density function directly.

Measurements have been conducted at low temperature in the solid state with a well-characterized, inclusion-free sample. Magnetic field-cycling NMR techniques have been used to record the spin-lattice relaxation rate $T_1^{-1}(\omega)$ as a function of the B field. These were based on the saturation-recovery sequence in pulsed NMR; the techniques and apparatus have been described elsewhere (*6*). The B-field dependence of $T_1^{-1}(\omega)$ in calix[4]arene recorded at three temperatures is shown in Fig. 2A. In all three spectra, the most important feature is the peak centered at $B = 0.82$ T corresponding to frequency $\gamma B/2\pi = 35$ MHz. This peak grows in amplitude with increasing T and is the feature of principal interest to this report. Additional components centered at zero frequency and related to stochastic dynamics are also exhibited in the spectra.

Peaks in $T_1^{-1}(\omega)$ that are offset from zero frequency can arise from (i) zero-field splittings associated with magnetic interactions and (ii) coherent molecular tunneling dynamics. The calix[4]arene molecule contains only carbon, oxygen, and hydrogen atoms. None of the abundant nuclei with spin ½ and zero can give rise to a zero-field splitting of magnetic origin centered at 35 MHz. The quadrupolar nucleus ^{17}O has very low natural abundance (0.037%), and nuclear quadrupole resonance (NQR) frequencies in similar molecular environments revealed by $^1H-^{17}O$ cross relaxation (quadrupolar dips) are typically observed in the range 1 to 3 MHz (*7*, *8*). Similarly, NQR frequencies in deuterium are too small. By contrast, resonant relaxation driven at level crossings between nuclear spin and molecular tunneling states, as in the case of the methyl rotor (*9*), can be observed over a very wide range of frequency. The cage structure of the calixarene is quite rigid, and there are no side groups on the main skeletal framework that can exhibit rotational tunneling.

Coherent proton tunneling in the hydrogen bond network thus remains the only plausible origin of the peak observed. Indeed, incoherent proton tunneling dynamics have previously been observed in the H bonds of a closely related analog of this molecule (*10*), *p*-tert-butyl calix[4]arene (tBC). In that case, the dynamics were characteristic of motion in an asymmetric double-well potential (DWP), and strong coupling to the phonon bath, necessary to promote proton transfer, quenches the coherent tunneling modes. In circumstances where the potential is characterized by wells with equivalent energy, then the coupling to the environment is less strong and it is expected that coherent tunneling will persist. The isolated calix[4]arene molecule has high symmetry, and there are energetically equivalent tautomers associated with the possible proton positions in the hydrogen bonds. In the solid state, any nonequivalence in the tautomer energy arises from asymmetry in the crystal field, and this component can be small when the relevant intramolecular interactions that determine the potential energy landscape are small. We assign the relaxation peak centered at 0.82 T to coherent proton tunneling in the hydrogen bonds with tunneling frequency $\omega_t/2\pi = 35$ MHz.

The tunneling peak is absent in the spectral density at temperatures below 20 K, but its amplitude grows strongly with increasing temperature. Therefore, we propose that the coherent proton tunneling is associated with a moiety that becomes populated discernibly at temperatures above 30 K. The amplitude of the tunneling peak has been recorded at six temperatures in the range $30 \leq T \leq 80$ K (Fig. 2B; the upper temperature limit was imposed by the switching time of the magnet, which must be less than T_1). The growth closely follows a Boltzmann law with energy $D/k_B = (125 \pm 10)$ K.

The $T_1^{-1}(\omega)$ data revealed evidence for systematic peaks and troughs in the tunneling peak profile. To investigate this fine structure, we studied the peak with finer steps in magnetic field using an adaptation of the

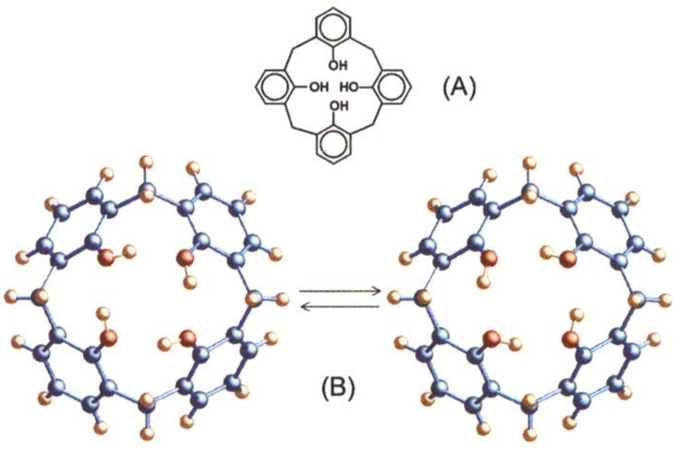

Fig. 1. Proton tunneling in calix[4]arene. (**A**) A schematic of the molecule. (**B**) The molecular structure showing the network of four H bonds at the base of the molecule and the two tautomers that can be interconverted by proton transfer. The heavy atom coordinates were determined by x-ray diffraction at ambient temperature. The proton positions are estimates based on difference maps and chemical constraints.

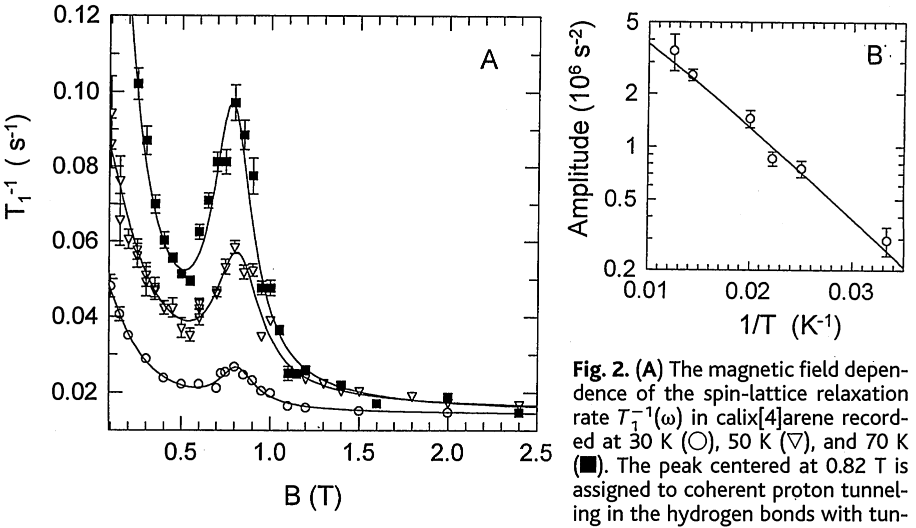

Fig. 2. (**A**) The magnetic field dependence of the spin-lattice relaxation rate $T_1^{-1}(\omega)$ in calix[4]arene recorded at 30 K (○), 50 K (▽), and 70 K (■). The peak centered at 0.82 T is assigned to coherent proton tunneling in the hydrogen bonds with tunneling frequency $\omega_t/2\pi = 35$ MHz. This feature in the spectral density is revealed at the level crossing where ω_t matches the proton Larmor frequency, ω_L. Additionally, there are spectral features centered at zero frequency associated with stochastic thermally activated processes; these are discussed in the text. (**B**) The temperature dependence of the coherent tunneling peak amplitude. The solid line is a fit to the Boltzmann function $\exp(-D/k_BT)/[1 + \exp(-D/k_BT)]$, with $D/k_B = (125 \pm 10)$ K. See text for details.

field-cycling NMR experiment that was originally developed for the study of rotational tunneling in symmetrical rotors (*9*). After saturation of the proton spin reservoir, the B field was rapidly switched to the region of interest, and the spin system was allowed to relax for 12 s. The partially recovered proton magnetization, M_z, was then recorded, and the sequence was repeated for selected B field values. Any field dependence in T_1 is revealed in the magnitude of M_z. The spectrum (Fig. 3) was recorded at 50.0 K and displays structure, notably the presence of outlying peaks.

If we assume that the dynamics are characteristic of a single hydrogen bond with a symmetric DWP, the eigenstates are characterized by symmetric and antisymmetric combinations of isolated well states. These are split by the tunneling splitting $\hbar\omega_t$. The hydrogen atom and its proton are delocalized between the two wells. We can write the space-spin eigenstates as $\psi_S\chi$ and $\psi_A\chi$, where χ represents the spin state of the proton; these have energy $(-\tfrac{1}{2}\hbar\omega_t \pm \tfrac{1}{2}\hbar\omega_L)$ and $(+\tfrac{1}{2}\hbar\omega_t \pm \tfrac{1}{2}\hbar\omega_L)$, respectively. A level (anti) crossing can be identified when $\omega_t = \omega_L$, and the dipolar interaction with a nearby spectator proton, rendered time-dependent by the motion, drives transitions involving a change in tunneling state simultaneously with a single proton spin flip. This resonant relaxation term is analogous to those that appear in the $T_1^{-1}(\omega)$ expressions for methyl tunneling (*9*, *11*) and can be identified as the origin of the peak in the spin-lattice relaxation rate centered at the tunneling frequency. Additionally, in the general case, one may expect to observe two-proton spin flip transitions when $\omega_t/2 = \omega_L$, but these are evidently not observed with measurable intensity in our experiments. It is not unusual in methyl tunneling for spectral features to be absent at some level crossings. In this system, it is possible that the coherent peak corresponds to $\omega_t/2 = \omega_L$, but given that there are twice as many states involved with the primary level crossing, we propose that the assignment $\omega_t = \omega_L$ is more likely. The transition probabilities will be the subject of future experimental and theoretical studies.

In writing the eigenfunctions for the system comprising the network of four equivalent H bonds, the indistinguishability of the four protons must be taken into account. Therefore, if the spatial eigenstates for each H bond are written as ψ_k ($k = A,S$) as above, then linear combinations of product states for the spatial degrees of freedom comprising terms such as $\psi_k^{(1)}\psi_k^{(2)}\psi_k^{(3)}\psi_k^{(4)}$ must be constructed that are either symmetrical or antisymmetrical with respect to particle exchange; this also applies to the spin functions that describe the four protons. So that the total eigenfunction is compatible with the exclusion principle, the symmetrical spatial eigenfunctions are combined with antisymmetrical spin eigenfunctions to construct a space-spin eigenfunction; similarly, antisymmetrical spatial eigenfunctions are combined with symmetrical spin eigenfunctions. Therefore, we identify spin 2, 1, and 0 eigenstates for the network comprising four H bonds. In the case where the coupling between hydrogen bonds is zero, these will be degenerate, but when there is a finite tunneling matrix element associated with interacting H bonds, this will give rise to a splitting J between the spin-0, spin-1, and spin-2 species. There are two types of tunneling matrix element describing the interactions among the four H bonds, one describing the coupling of adjacent H bonds and a second describing coupling across the square. The precise splitting pattern will depend on the magnitudes of these two.

A feasible energy level diagram for the H bond network is sketched in Fig. 4. The region around $\omega_t = \omega_L$ is of particular interest. The coupling between H bonds introduces structure into the level-crossing spectrum; a number of one-spin and two-spin level (anti) crossings that involve a simultaneous change in tunneling state are identified. The resulting spectrum deduced from this diagram is superimposed on the experimental level-crossing spectrum (Fig. 3). With a value of 3 MHz for the coupling J between H bonds, satisfactory agreement with the experimental spectrum is obtained, although a full quantitative analysis will be the subject of future theoretical modeling.

Certainly it is to be expected that coupling will be manifest because elementary consideration of the bonding in the network will lead to the conclusion that the dynamics of one H bond must be influenced by the proton motion in an adjacent H bond. Indeed, the extent to which the motion of the four protons is a concerted or step-wise process is a matter of topical interest in the context of the mechanisms of proton transfer (*12*, *13*). In this particular case, the protons are delocalized and the dynamics are purely quantum mechanical so the system can provide fundamental insight into a subject that is

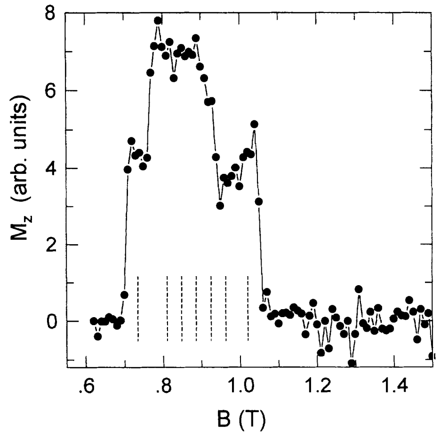

Fig. 3. The level-crossing spectrum in calix[4]arene recorded at 50.0 K; the partially recovered proton magnetization M_z reveals the magnetic field dependence of the spin-lattice relaxation rate. A linear background has been subtracted. This scan reveals structure in the tunneling peak that is assigned to coupling between the H bonds in the network. The dashed lines show the positions of various level crossings predicted by the energy level diagram in Fig. 4 assuming the coupling frequency ω_{coup} = 3 MHz.

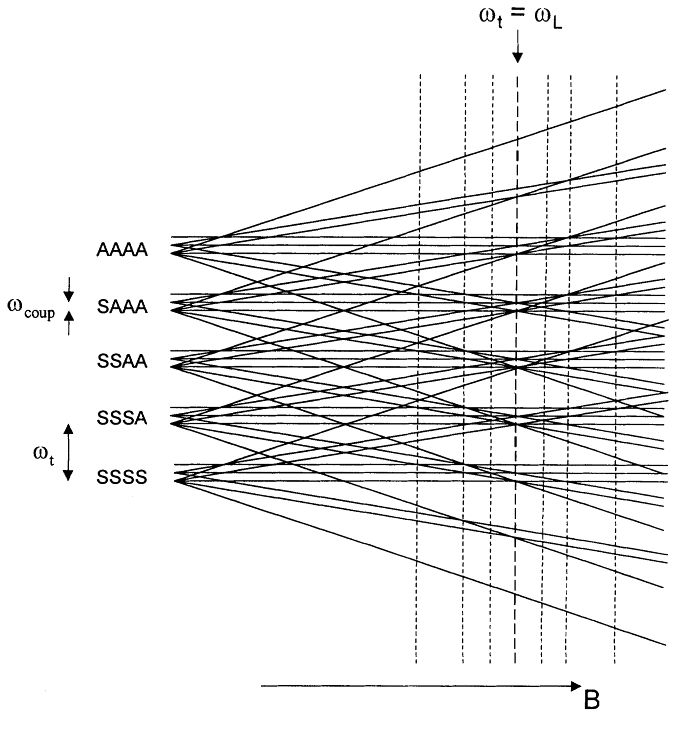

Fig. 4. An energy level diagram for four coupled H bonds showing the magnetic field dependence (not to scale). The possible ground state eigenfunctions of a single H bond are ψ_S and ψ_A with splitting $\hbar\omega_t$. Introduction of coupling between H bonds raises the degeneracy of spin 2, 1, and 0 species. The coupling is characterized by the splitting $\hbar\omega_{coup}$.

often formulated in the context of classical mechanics. To elucidate further the mechanisms of proton motion, future investigations of this system will be undertaken on deuterated analogs.

That the moiety that displays coherent proton tunneling is not the ground state of the system is of interest and worthy of further examination. The energy characterizing the growth of the tunneling peak, $D = (125 \pm 10)k_B$ K, is relatively small and of similar magnitude to the energy differences between tautomers related, for example, by proton transfer in carboxylic acid dimers and in the closely related molecule tBC (*10*). Examination of the spectral density recorded on calix[4]arene as in Fig. 2A reveals the presence of two identifiable incoherent components related to thermally activated stochastic proton-hopping processes. One of these, which we shall label process 1, has characteristics analogous to the proton transfer process reported in earlier observations in tBC and is modeled well by incoherent proton tunneling in a DWP with asymmetry *D*. Therefore, we propose that process 1 is the mechanism by which the moiety that exhibits coherent tunneling becomes populated. One way this can be realized is if the potential energy surface related to proton transfer in a particular molecule is influenced by the tautomeric state of its neighboring molecules. As neighboring molecules undergo incoherent tunneling with fast exchange on the time scale of ω_t, and as the temperature becomes sufficiently high to substantially populate both wells of the neighbor's asymmetric DWP, so the asymmetry for the moiety in question may become close to zero and permit the coherent tunneling processes we observe to mediate proton transfer. Precedence for this model is provided by the distortion of the crystal field that arises from the introduction of optical probe molecules in benzoic acid (*14*), although in that case, the distortions are static.

The second incoherent thermally activated proton-hopping process observed, which we shall label process 2, is much slower, with classical Arrhenius behavior described by correlation time $\tau_c = 1.2 \times 10^{-12} \exp(900/T)$s. The activation energy is $\Delta E_{act}/k_B = 900$ K, and it is proposed that this process may be assigned to rotational flips of the O-H groups, giving rise to H bond flip-flop motion of the kind advocated by Saenger *et al.* (*15*) and observed by Bernhard *et al.* in Dianin's compound (*16*). Additional experiments will be required to investigate this process, but in our data, it appears to be independent and separate from the coherent tunneling motion.

The observation of discrete tunneling frequencies associated with translational atomic displacements is rare. Tunneling associated with proton transfer in H bonds has been observed by microwave spectroscopy in the gas phase where the molecules are well isolated (*17*). In the solid state, coherent tunneling associated with proton transfer has been uniquely observed in doped benzoic acid where optical probes in low concentration introduce a crystal field distortion for a shell of molecules in the immediate vicinity that is just sufficient to offset the energy asymmetry characteristic of the bulk material; the tunneling frequency is 8.4 GHz (*14*). In this report, we have described coherent proton tunneling with a frequency of 35 MHz in a hydrogen bond network; also important is the coupling between hydrogen bonds that the spectra reveal. These findings will be important both to our understanding of processes relevant to the life sciences and to the fundamental role played by tunneling in chemical dynamics.

References and Notes

1. A. Kohen, R. Cannio, S. Bartolucci, J. P. Klinman, *Nature* **399**, 496 (1999).
2. N. S. Scrutton, J. Basran, M. J. Sutcliffe, *Eur. J. Biochem.* **264**, 666 (1999).
3. D. Diamond, M. A. McKervey, *Chem. Soc. Rev.* **25**, 15 (1996).
4. N. Bloembergen, E. M. Purcell, R. V. Pound, *Phys. Rev.* **73**, 679 (1948).
5. R. Kubo, K. Tomita, *J. Phys. Soc. Jpn.* **9**, 888 (1954).
6. D. F. Brougham, A. J. Horsewill, R. I. Jenkinson, *Chem. Phys. Lett.* **272**, 69 (1997).
7. C. P. Cheng, T. L. Brown, *J. Am. Chem. Soc.* **101**, 2327 (1979).
8. M. Torkar, V. Zagar, J. Seliger, *J. Magn. Reson.* **144**, 13 (2000).
9. A. J. Horsewill, *Prog. Nuclear Magn. Reson. Spectrosc.* **35**, 359 (1999).
10. D. F. Brougham, R. Caciuffo, A. J. Horsewill, *Nature* **397**, 241 (1999).
11. J. Haupt, *Z. Naturforsch.* **26a**, 1578 (1971).
12. F. Aguilar-Parrilla *et al.*, *J. Am. Chem. Soc.* **114**, 9657 (1992).
13. J. L. G. de Paz *et al.*, *J. Chem. Soc. Perkin Trans.* **2**, 101 (1997).
14. A. Oppenländer, Ch. Rambaud, H. P. Trommsdorff, J. C. Vial, *Phys. Rev. Lett.* **63**, 1432 (1989).
15. W. Saenger, Ch. Betzel, B. Hingerty, G. M. Brown, *Nature* **296**, 581 (1982).
16. T. Bernhard, H. Zimmerman, U. Haeberlen, *J. Chem. Phys.* **92**, 2178 (1990).
17. S. L. Baughcum, R. W. Duerst, W. F. Rowe, Z. Smith, E. B. Wilson, *J. Am. Chem. Soc.* **103**, 6296 (1981).

18. N.H.J. is sponsored by an Engineering and Physical Sciences Research Council postgraduate research scholarship. We are grateful to F. Ugozzoli for preparing the sample and for discussions with M. E. Smith.

8 September 2000; accepted 20 November 2000

Photoactivated Fluorescence from Individual Silver Nanoclusters

Lynn A. Peyser, Amy E. Vinson, Andrew P. Bartko, Robert M. Dickson*

Fluorescence microscopy of nanoscale silver oxide (Ag_2O) reveals strong photoactivated emission for excitation wavelengths shorter than 520 nanometers. Although blinking and characteristic emission patterns demonstrate single-nanoparticle observation, large-scale dynamic color changes were also observed, even from the same nanoparticle. Identical behavior was observed in oxidized thin silver films that enable Ag_2O particles to grow at high density from silver islands. Data were readily written to these films with blue excitation; stored data could be nondestructively read with the strong red fluorescence resulting from green (wavelengths longer than 520 nanometers) excitation. The individual luminescent species are thought to be silver nanoclusters that are photochemically generated from the oxide.

The strength of nanoparticle absorption and emission enables facile observation of single particles (*1, 2*) with much higher and often more robust signals than those produced by organic dyes (*3–5*). Such single-particle observations have furthered understandings of heterogeneity in molecular behavior (*6–8*). Complementary to environment-influenced single-molecule dynamics (*5, 7*), nanoparticles are larger, more complex systems, and their fluorescence often reflects the nanoparticle/surface interactions that affect electron-hole recombination (*1, 2*). However, the utility of nanoparticles would be greatly enhanced if their fluorescence were designed to be "caged" or photoactivated. Such caged fluorescent particles could be rapidly switched on and used, for example, as nanoscopic optical storage elements or as probes in living systems. Although photochromic molecules have been observed as single fluorescent entities (*6*), to date no photoactivated fluorescent nanoparticles have been produced to the best of our knowledge, let alone ones that are observable on a single-particle level. Such caged fluorescence should prove easier to observe from small clusters that are photochemically generated from, yet stabilized by, a surrounding solid

---

School of Chemistry and Biochemistry, Georgia Institute of Technology, Atlanta, GA 30332-0400, USA.

*To whom correspondence should be addressed. E-mail: dickson@chemistry.gatech.edu